Thin-Walled Structures 117 (2017) 367–377

Contents lists available at ScienceDirect

Thin-Walled Structures

journal homepage: www.elsevier.com/locate/tws

Full length article

Model reduction in thin-walled open-section composite beams using Variational Asymptotic Method. Part II: Applications

Dineshkumar Harursampath[a], Ajay B. Harish[b,*], Dewey H. Hodges[c]

[a] Dept. of Aerospace Engineering, Indian Institute of Science, Bangalore 560012, India
[b] Institute of Continuum Mechanics, Leibniz Universität Hannover, Appelstr. 11, Hannover 30167, Germany
[c] Daniel Guggenheim School of Aerospace Engineering, Georgia Institute of Technology, Atlanta, GA 30332, USA

ARTICLE INFO

Keywords:
Anisotropic
Asymptotic
Beam
Bending
Cantilever
Composite materials
Fiber reinforced
Laminated
Stochastic
Warping
Thin-walled
Open-section
Variational Asymptotic Method
Trapeze effect
Vlasov effect
Contact

ABSTRACT

This part of the work describes applications of a comprehensive and reliable tool for analysis of thin-walled, open-section composite beams. The developed comprehensive and reliable tool is used for analysis of commonly used cross sections (I-, C-, Z-, and star) of thin-walled open-section composite beams. Usage of VAM renders a rigorous asymptotically correct reduction of the 3-D nonlinear problem to a much simpler 1-D nonlinear problem, with closed-form solutions contributing to rapid yet accurate analysis. This computational efficiency is demonstrated through a Monte-Carlo-type stochastic analysis.

1. Introduction

Thin-walled composite beams are commonly employed in various industries owing to their superior properties, such as high stiffness and strength-to-weight ratios. Despite their superior properties, they exhibit complicated material behavior due to several nonlinear and non-classical effects (such as Trapeze, Brazier, and Vlasov effects) that are commonly observed during operations. Such complicated phenomenon cannot be easily captured by classical tools. Experimental techniques or simple beam models (with assumed factor-of-safety) drives up the overall design and development costs, thus not allowing thin-walled, open-section beams to be exploited to their potential. This necessitates fast yet accurate tools that can be used during preliminary design stages.

Owing to standardization of the Finite Element Method (FEM), 3D FEM solutions can be considered as a basis for comparison for other numerical solution techniques. However, 3D FEM for general design and analysis can be computationally cumbersome and expensive. For example, consider an I-section beam with dimensions 2.5 m in length, 50 mm in breadth and 50 mm in height. The web and flanges each comprise of 16 plies with thickness of each ply being 0.13 mm. Being a bending dominated problem, a FEM mesh with tri-linear displacement elements (or linear 8-noded hexahedrons) can result in numerical problems such as locking. Thus, an ideal element for meshing could be the tri-quadratic displacement elements (or quadratic 20-noded hexahedrons). Considering two elements along the thickness of the beam results in 406,908 elements (C3D20 from Abaqus) and 2,198,658 nodes. Consideration of solid elements with 3 degrees of freedom (dof's) or unknowns per node implies 6,595,974 dof's or unknowns. Now, if the problem is multi-physics in nature, including more dof's per node, such as temperature or non-local damage, this would drastically increase the size of the problem. Solving such systems can require parallel computing facilities, parallel solvers etc alongside long computational time for each simulation. Computing on 32-processors (single-node) of a Xeon E5 cluster and using approximately 250 GB of memory will require more than 96 h of computing time. In contrast, comparable results can

* Corresponding author.
E-mail addresses: dinesh@aero.iisc.ernet.in (D. Harursampath), harish@ikm.uni-hannover.de (A.B. Harish), dhodges@gatech.edu (D.H. Hodges).

http://dx.doi.org/10.1016/j.tws.2017.03.021
Received 28 October 2015; Received in revised form 18 December 2016; Accepted 14 March 2017
Available online 28 March 2017

be computed using a reduced-order model obtained from the VAM (i.e., the framework that is the subject under discussion in this paper) in less than a minute on a simple Dual Core laptop.

In addition, laminated composites have inherent uncertainties originating both in their manufacturing processes as well as service lives and their properties generally have significant scatter around the mean value. Thus, the uncertainties in material and geometric properties must be considered in the analysis. Almost all previous approaches in the literature that employ VAM for dimensional reduction simplify the problem by considering the uncertain parameters as deterministic and account for uncertainties using empirical safety factors in design. Exceptions include works of Li [37] and Murugan et al. [39]. However, the conventional deterministic approach is not appropriate for realistic applications. Thus, it is required that the deterministic design be expanded to account for these uncertainties. A simple Monte-Carlo evaluation of even small sample sizes of few tens of samples could be infeasible using 3D FEM solutions.

Alternatively, there have been several approaches and tools developed for analysis of thin-walled, open-section beams including for post-buckling behavior. Most common ones include analytical beam theories (generally restricted to isotropic materials) or FEM-based beam models such as generalized beam theory. Yet, most of these models are not always directly capable of capturing all the nonlinear and non-classical effects that arise in thin-walled beams. Thus, the current work is motivated by the need for a general purpose tool to capture the overall behavior, including non-classical effects of thin-walled, open-section composite beams in a fast yet accurate manner. This is partly because it is feasible in the asymptotic framework to obtain approximate closed-form solutions. This work is implemented using MATLAB (and compatible for usage with open-source SciLab) to visualize non-classical, nonlinear effects and to enable multi-objective tailoring of composite beams with varying layups. In this work, the applicability of the developed theory to a wide variety of commonly favored aerospace structures (with cross sections such as I-sections, T-sections, X-sections, Z-sections, cruciforms, and stars), all of which may be constructed as an assembly of strip-like beams, is demonstrated. This work also considers the random nature of material properties, and the probabilistic perspective provided by the current model enables one to quantify some of the many inherent uncertainties in composite beams.

Overall, this work provides an effective mathematical tool for analysis of open-section thin-walled composite beams and could assist in composite tailoring of a variety of layups and cross-sectional shapes. This also accounts for the generality of the layup and random fluctuations of input parameters, thus providing a reliable and computationally efficient probabilistic model. Also considered is the generality of the shape as well as the number and orientation of the strips forming the open-section beam. This renders the tool versatile for composite tailoring of almost all commonly employed forms of open-section beams. In this work, the developed tool will be demonstrated for applicability for different cross sections and validated with results from the literature and 3-D FEM.

2. Review of earlier works

This section provides a brief literature review of tools developed (including FEM-based beam models, analytical approaches) to model thin-walled, open-section beams. There have been many studies, particularly pertaining to civil engineering applications, where thin-walled members are used in steel structures and concrete bridges. For practical purposes, isotropic material models are generally assumed in the analysis and design of these structures. Some of the main issues addressed in these works include those pertaining to effect of distortional loading and cross-sectional warping [10], and are based on or follow the ideas expressed by Vlasov [54]. Several analytical and finite element formulations, such as [1,4,59,32], have been developed based on the work of [54]. Along the same direction, [34] considered a FEM formulation to account for warping effect through a Total Lagrangian formulation, while [44,51] considered higher-order terms stemming from the rotation matrix.

One of the common approaches has been to formulate beam elements in an FEM framework. Giavotto et al. [22] applied discretization of displacement fields using planar elements, and this methodology was further applied in cross-sectional analysis [5], optimization [9,7], and fracture [8] of wind turbine blades made of composite materials using the open-source code BECAS. The idea was also further applied by Høgsberg and Krenk [29] for moderately thin-walled cross sections using higher-order isoparametric elements into a Matlab-based FEM framework called BeamSec. In spite of the discussion regarding the generality of the developed formulations, the ability of the methodology to capture the nonlinear and non-classical effects in thin-walled open-section beams is yet to be demonstrated. Similar higher-order isoparametric elements have been developed in several works, like [50,47,38], with a goal to accurately capture torsion and shear fields.

Another method had been the generalized beam theory approach for FEM models. Original equations developed by Schrad [46] were valid for small deformation and moderate rotation. This has been further extended by Silvestre and Camotim [48] to provide a nonlinear GBT formulation and by Basaglia et al. [2] for moderate to large rotation – thus making it feasible for post-buckling analysis for arbitrary load conditions.

Some of the latest works using FEM for modeling thin-walled composite structures include series of papers by Genoese et al. [21,20], Garceaa et al. [19], Gabriele et al. [18], Nguyen et al. [40]. Genoese et al. [21] proposes a mixed linear model based on Hellinger-Reissner mixed variational principle for heterogeneous materials, including warping and section distortions. In addition, Blasques et al. [6] demonstrate methodology for the usage of constraint equations to impose free and restrained warping conditions and the same has been used in this work.

There have been several other isolated works studying thin-walled, open-section beams using FEM-based beam models under various subtopics, such as symmetric, fiber-reinforced laminates [3,58], optimization [30,15,52,53,11], torsional analysis [35,31,55,13], distortion mechanics [49,23], shear deformability [16], and general nonlinear elements [24,42,56]. There have been several analytical solutions as well but mostly addressing isotropic materials. Lee and Lee [36] develop an analytical approach to capture the flexural-torsional behavior of thin-walled, open-section composite beams and demonstrated its application to I-section beams. But none of the other known works address the issues concerning composite or anisotropic materials.

In recent years the Variational-Asymptotic Beam Section (VABS) analysis, originally developed by Cesnik and Hodges [12] and Yu et al. [62] based on the principles of Variational Asymptotic Method (VAM), has been widely used for modeling composite structures. Yu et al. [63] discuss the history and capabilities of VABS, which was validated for different classes of beams. Kovvali and Hodges [33] extend VABS functionalities to model pretwisted and curved beams comparing the results with commercial software with regard to both the dynamic behavior (resulting natural frequencies) and static deflections. Yu et al. [61] discuss the recent updates to VABS which include consideration of the effects of applied loads in cross-sectional analysis and constraints on warping based on 1-D displacements and rotations. Lately, VABS is also available as a cloud-variant on cdmhub.org.

VABS already treats nonlinear and non-classical effects in thin-walled open-section composite beams using VAM but implemented in a FE framework. In other words, VABS already treats the Vlasov and Trapeze effects that are of importance in thin-walled open-section beams. However, unlike analytical solutions discussed here, VABS uses FE-based method for the cross-sectional analysis. In addition, VABS requires a separate 1-D tool (like GEBT) for usage of cross-sectional results to obtain actual beam deflections and rotations. A discussion of the start-of-the-art in nonlinear composite beam modeling can be found

in the book by Hodges [26]. Like VABS, the current work also enables a two-way interaction between the 2-D cross-sectional and the global 1-D beam analyses. In comparison to the work of Popescu and Hodges [45], which still forms the basis for the nonlinear analysis of VABS, the closed-form solutions discussed in the work of Hodges et al. [27], which forms the foundation of the current work captures many more terms. In particular, the asymptotically-correct first-order strain energy per unit length of a strip is quartic in the 1-D generalized strains as shown in the work of Hodges et al. [27]. However, VABS can currently deal only with a strain energy density which is cubic in the 1-D generalized strains. Using Hodges et al. [27] as a building block, the current work can in general, generate terms, in addition to those already included in VABS, but of equal importance. For the strip, these additional terms are associated not only with torsion but also with flap wise bending and their couplings with each other and other 1-D strains. However, for thin-walled open sections constructed as an assembly of the strips, only the nonlinear terms associated with torsion remain important, as demonstrated in Part-I. Additionally, the present work demonstrates a computational advantage over VABS, both in the calculation of the 1-D stiffness and the 3-D recovery, owing to the former's closed-form analytical framework as compared to the latter's dependence on a finite element based numerical framework. The present work can also, by itself, be a complementary addition to the existing VABS framework for special cases. VABS, however, remains a much more general purpose analysis tool due to its ability to deal with any complicated cross-sectional geometry and/or material distribution.

Alongside VABS, several other approaches have been used in the literature for modeling slender structures, including Geometrically Exact Beam Theory (GEBT) by Yu and Blair [60], proposed as a general-purpose tool for nonlinear analysis of 1-D composite structures. However, it is imperative to note that most of the works deal with isotropic structures while only few both deal with a general layup configuration and consider nonlinear couplings as well.

3. Application to common cross sections

The developed reduced-order model is implemented in MATLAB as an interactive analysis called Open Section Beam Analyzer (OSBA). It is capable of processing the user input on the beam type and related geometric and material properties, and provides stiffness matrices and warping solutions. The developed analysis can be user-defined to provide either a deterministic or a probabilistic solution (through simple Monte Carlo simulations). In this section, the developed theory is applied to I-sections which are commonly used in several civil and aerospace engineering applications. The solutions from OSBA are validated by comparison with 3-D FEM, shell-based FEM solutions obtained from Abaqus, and results available in the literature. Following this other commonly used cross sections, such as star- and Z-section beams, are discussed and compared with results available in the literature.

3.1. I-section beams

Consider a pretwisted I-section beam with three uniform but generally anisotropic layups, one throughout each component strip. Fig. 1 shows the cross section. The beam reference line is taken to pass through the center of web, and not the centroid, to demonstrate the flexibility of the developed method in choosing the cross-sectional reference point. The composite layups are considered to be made of glass-epoxy and the material properties of each lamina is considered as $E_L = 53.78$ GPa, $E_T = 17.93$ GPa, $G_{LT} = 8.96$ GPa and $\nu_{LT} = 0.25$. The total length of the beam is taken as 2.5 m. The width of the flanges and web is 50 mm, and the thickness of each ply is 0.13 mm. The pretwist of the beam (k_1) is zero and each of the flanges and web is comprised of 16 plies.

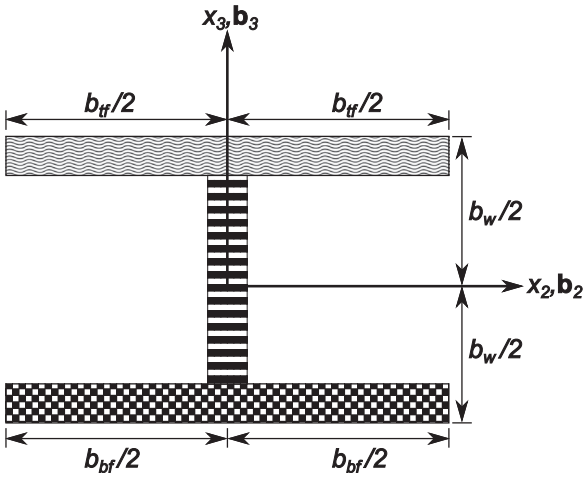

Fig. 1. Desired I-beam configuration.

3.1.1. Comparison with literature and shell-based FEM: symmetric layups

In order to validate the developed model, the I-section beam was analyzed in Abaqus CAE using the conventional shell element and composite layup tool as shown in Fig. 2. The I-section beam was meshed with 15,531 nodes and 15,000 S8R shell elements, thus requiring solution of a system with 93,186 degrees of freedom (d.o.f).

The deflections and rotations are measured at a point on the tip of the beam that corresponds to the intersection of the center line and free end of the beam. In Table 4 of Vo and Lee [57], deflections obtained from Abaqus element S9R5 are compared with results obtained from the nonlinear beam element proposed in their own work. In Table 1, we compare the deflections obtained from OSBA and Abaqus (using S8R shell elements) with the published results of Vo and Lee [57]. The Abaqus model provides a suitable benchmark with respect to which the OSBA results can be compared and thus validated.

For different layups (as in Table 1), a load of 250 N is applied along the negative x_3-axis at the free end of the beam and the resulting deflections and rotations are calculated. The deflections u_3 from S8R Abaqus element used in this work and from OSBA match reasonably well with the results presented by Vo and Lee [57]. However, it is important to clarify that the bending (about x_3) and axial displacements from both OSBA and S8R element of Abaqus were nearly zero in comparison to the non-zero bending and axial displacement presented by Vo and Lee [57]. The Abaqus S9R5 element has more degrees of freedom compared to the S8R shell element used here, and these inherently different formulations are known to lead to slightly different results. It is also important to note that the S8R5 elements are available by default in Abaqus but not the S9R5 elements. Extra pre-processing is necessary to add middle nodes to the S8R5 elements. Finally, as will be discussed later in more detail in the case of Z-section beams as well as in Vo and Lee [57], there is an uncertainty in modeling the exact nature of boundary conditions at the free end, which also contributes to some variation in the results.

3.1.2. Comparison shell-based FEM: random layups

In this section, building on earlier comparisons with shell-based results, the load-deflection behavior for a more general layup as in Fig. 3, such that the coupling terms of the stiffness matrix are non-zero, is presented. A full 3-D FEM simulation would be necessary to accurately capture all the warping effects. However, considering the thickness-to-length ratio of the beam to be very small, a very fine mesh would be required to obtain accurate results. Assuming at least two elements through the thickness and a uniform mesh would lead to approximately 250,000 hexahedral elements per flange or about 750,000 elements (i.e., about 6 million d.o.f, for the entire beam). Since the problem is bending dominated, the ideal choice would be 20-

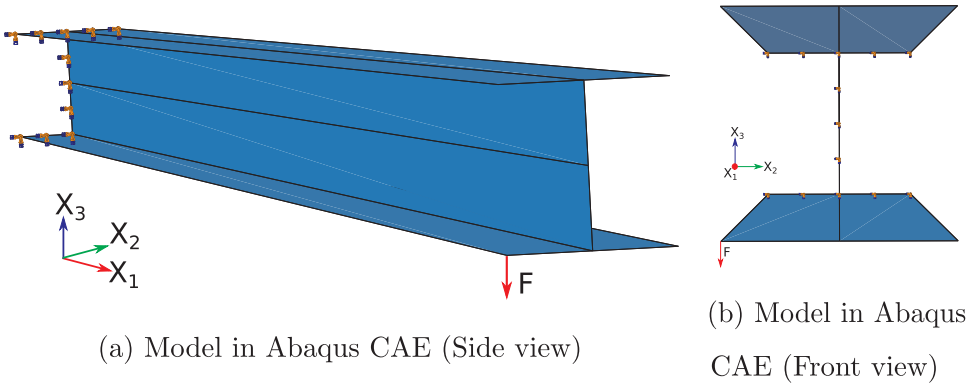

Fig. 2. Model in Abaqus CAE 6.13 using conventional shell elements (middle & right) (a) Model in Abaqus CAE (Side view). (b) Model in Abaqus CAE (Front view).

Table 1
Deflections u_3 (in cm) of a cantilever composite I-section beam with symmetric angle-ply laminates in the flanges and web under a load of 250 N at the free end.

Layup	Present Work		Vo and Lee [57]	
	Abaqus (S8R)	OSBA	Abaqus (S9R5)	FEM
$[0/90]_{4\,s}$	23.8798	23.8186	23.6829	23.783
$[90/-90]_{4\,s}$	47.9277	47.8816	46.2755	46.7453
$[75/-75]_{4\,s}$	47.1841	47.1564	45.6077	46.0678
$[60/-60]_{4\,s}$	43.4339	43.4438	42.2037	42.5798
$[45/-45]_{4\,s}$	34.3499	34.3741	33.7463	33.9294
$[30/-30]_{4\,s}$	23.8062	23.7952	23.6133	23.6384
$[15/-15]_{4\,s}$	17.717	17.6689	17.6434	17.6002
$[0]_{16}$	16.0284	15.9635	15.976	15.9113

noded hexahedral (or tri-quadratic) elements or, better yet, using more elements through the thickness. Both these alternatives will only add more d.o.f to the already computationally expensive problem. Thus, standard shell elements (such as S8R and S8R5) present a more efficient way to obtain order-of-magnitude estimates for secondary deflections and rotations, and measures of primary deflections and rotations, which would be sufficient for preliminary design. Thus, in this work, results using Shell elements in Abaqus are used for comparison. For a vertical load as applied earlier, secondary deflections and rotations would be U_2, θ_1, and primary deflections and rotations are U_3 and θ_2.

Vertical loads are applied at the right tip of the bottom flange along the negative x_3-direction, as shown in Fig. 2. The simulations are quasi-static in nature and the magnitude of the load is varied, for each simulation, with an increment of 25 N. The loads, thus, applied are 25 N, 50 N, 75 N, …, 225 N, 250 N. A total of eleven simulations, each at different load magnitude, are performed to obtain the tip displacements and rotations. The resulting deflections and rotations are plotted as a function of applied load in Figs. 4 and 5, respectively.

Since the standard Abaqus shell elements are better for modeling thick shells than they are for thin shells, they do not show the significant warping effects that would be otherwise seen at the free end. Thus, comparison of results for the restrained warping condition for the free end would be the best to compare with Abaqus results. As can be seen in Figs. 4 and 5, the primary deflections and rotations (namely U_3 and θ_2) resulting from the applied load and obtained from OSBA are in excellent agreement with results obtained from Abaqus shell elements. These primary deflections and rotations are almost independent of the boundary conditions applied. These results constitute a source for validating primary deflections and rotations.

Since Abaqus does not allow imposition of warping restrain through the standard boundary conditions / load options, alternative methods have been used to check the comparability between the solutions. As imposed in the work of Blasques et al. [6], kinematic and distributive constraints are also considered alongside a third alternative where θ_3 is imposed on the free surface. Imposition of zero-value of θ_3 on the free surface also results in $U_1 \approx 0$ and the same is seen to be true when kinematic or distributive constraints are imposed. The nearest approximation, constraining θ_3 to be zero matches well with results obtained from OSBA. Restricting the warping at the free end also constrains the axial deformation (U_1) at the free end, which is negligibly small of order 10^{-5} m, with good agreement between Abaqus and OSBA. The secondary deflection U_2 and rotation θ_1 also show reasonable agreement. It should be noted here, that constraining $\theta_3 = 0$ leads to better approximation of U_2 while kinematic constraints better approximate θ_1. The difference between the boundary conditions is the only possible rationale to explain the difference between tip rotations, namely θ_1. The resulting differences will again be discussed in the upcoming subsection on comparison for Z-section beams. Thus, overall OSBA

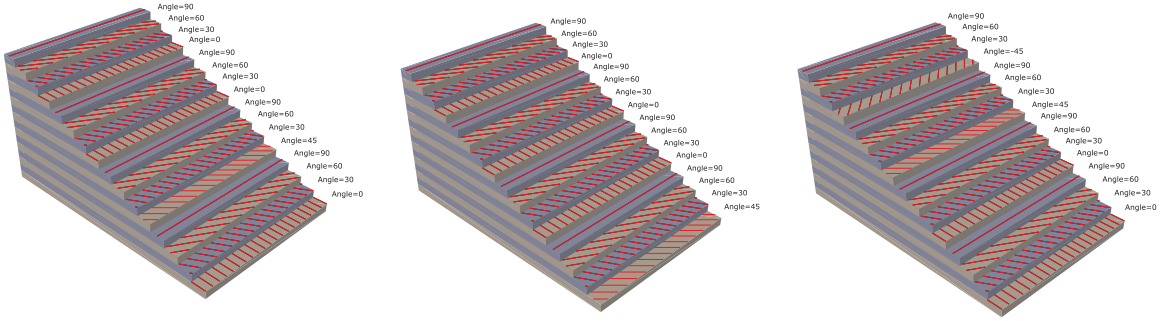

Fig. 3. Ply stack of flanges and web of the I-section beam (a) Ply stack of bottom flange. (b) Ply stack of top flange. (c) Ply stack of web.

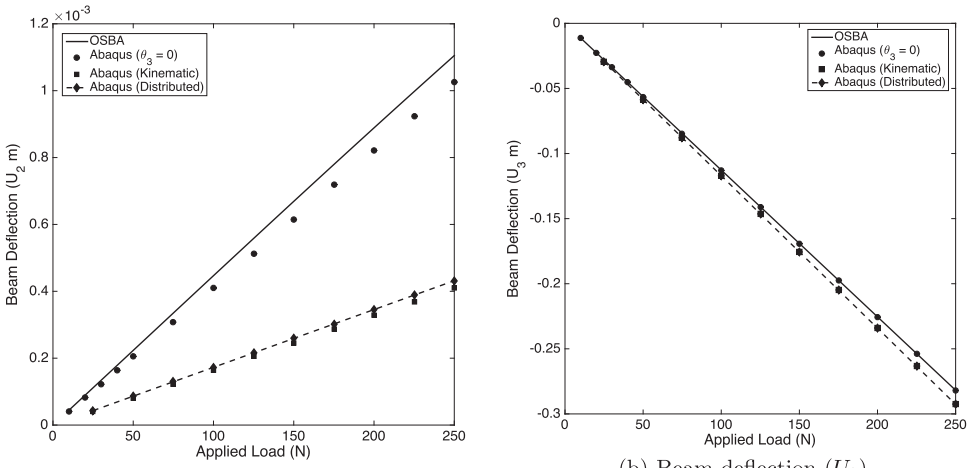

(a) Beam deflection (U_2) (b) Beam deflection (U_3)

Fig. 4. Primary beam tip deflections (Comparison of results from OSBA and Abaqus) The Abaqus results shown here have three different boundary conditions at the free end: $U_1 = 0$, Kinematic constraint on free face, Distributed constraint on free face (a) Beam deflection (U_2). (b) Beam deflection (U_3).

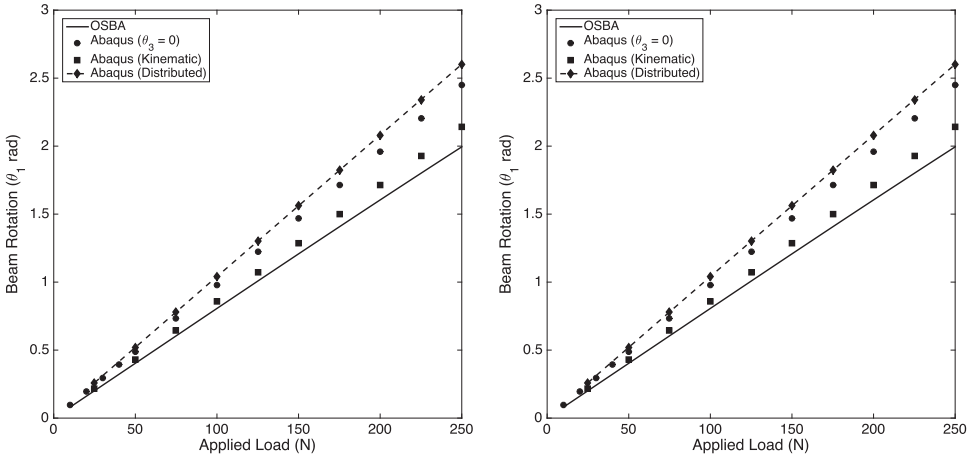

(a) Beam rotation (θ_1) (b) Beam rotation (θ_2)

Fig. 5. Primary beam tip rotations (Comparison of results from OSBA and Abaqus) The Abaqus results shown here have three different boundary conditions at the free end: $U_1 = 0$, Kinematic constraint on free face, Distributed constraint on free face (a) Beam rotation (θ_1). (b) Beam rotation (θ_2).

accurately estimates the primary deflections and rotations at a significantly smaller computational cost.

3.2. Applications to star beams

Francois [17] proposes many applications for so-called star beams. These beams present a very peculiar situation, one that is shared with strip-beams. Among the nonclassical effects, end effects are not important but nonlinearities are crucial. The leading stiffness coefficient associated with end effects, S_{66}, is dependent on constants c_n, as described in Eq. (10) of Part-I. Reproducing Eq. (11) from Part-I,

$$\begin{aligned}\sum_{n=1}^{N_s} b_n c_n &= c_p + x_{p2}(m)(\cos\alpha_p X_{p3} - \sin\alpha_p X_{p2}) \\ &= c_q + x_{q2}(m)(\cos\alpha_q X_{q3} - \sin\alpha_q X_{q2}) \\ &\quad (m = 1, \ldots, N_j)\end{aligned} \tag{1}$$

it can be inferred that the leading stiffness coefficient associated with end effects, S_{66} vanishes if and only if $c_n = 0$ and $\sin\alpha_n X_{n2} = \cos\alpha_n X_{n3}$ for $n = 1, 2, \ldots, N_s$. From Eq. (1), however, one sees that if the second of the above two conditions is satisfied, the first one gets satisfied automatically. For $\sin\alpha_n X_{n2} = \cos\alpha_n X_{n3}$ to hold for all the strips, when extrapolated, they should all pass through the reference point O about which the twist is defined. The best example for such a cross section would be a star section.

Results for the general star shape cross sections are presented and compared with the finite element and theoretical results of Dancila et al. [14] for star sections with 3, 4, and 6 component strips with antisymmetric layups. The formulation in this section does not apply to 2 component strips, because that case degenerates into a strip. Ironically, this is a much more complicated case for study because of nonlinearities from both flapwise bending and twist. Fig. 6 shows a star cross section with 6 component strips.

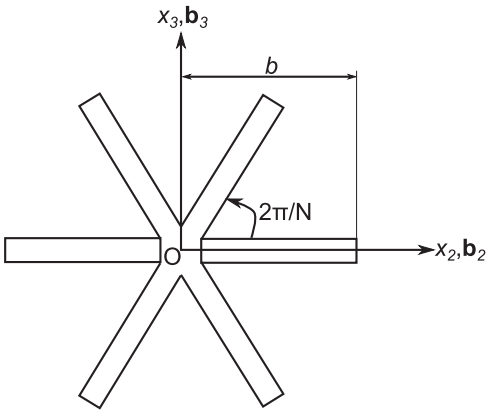

Fig. 6. Star beam.

For a star cross section comprised of $N \geq 3$ identical and equally spaced generally anisotropic strips, as shown for example in Fig. 6, the terms of the 1-D stiffness matrix is given by

$$
\begin{aligned}
S_{11} &= NbA \\
S_{12} = S_{21} &= \frac{N}{3}b^3Ak_1 - 2NbB \\
S_{15} = S_{51} &= \frac{N}{6}b^3A \\
S_{22} &= 4NbD - \frac{4}{3}Nb^3Bk_1 + \frac{N}{5}b^5Ak_1^2 \\
S_{25} = S_{52} &= \frac{N}{10}b^5Ak_1 - \frac{N}{3}b^3B \\
S_{33} = S_{44} &= \frac{N}{6}b^3A \\
S_{55} &= \frac{N}{20}b^5A
\end{aligned}
\tag{2}
$$

where the order of rows/columns is 1 – γ_{11}, 2 – κ_1, 3 – κ_2, 4 – κ_3 and 5 – ${\kappa_1}^2$, and $A = \overline{\overline{A}}_{11}$, $B = \overline{\overline{B}}_{16}$ and $D = \overline{\overline{D}}_{66}$ are stiffness properties of the component strips defined earlier in Eq. 12 of Part-I. Rest of the terms of the matrix are zeros. Note that bending in both directions is uncoupled from the rest of the problem, even for the generally anisotropic case. The nonlinear extension-twist problem, however, is fully coupled and is the source of the well-known trapeze effect.

Now, consider a pretwisted cantilevered star beam with a tip torque M_1 and a tip axial force F_1. The equilibrium equations are derived via the principle of virtual work. First, the strain energy is given as

$$
U = \int_0^l U_{1D}(\gamma_{11}, \kappa_1, \kappa_2, \kappa_3)dx_1 \tag{3}
$$

where the geometrically-exact strain measures for classical theory can be found, for example, in [28]. Both bending curvatures, κ_2 and κ_3, are zero because of their being decoupled from extension and twist, as described above. The geometrically-exact strain-displacement relations reduce to $\gamma_{11} = q'_1$ and $\kappa_1 = \theta'_1$ where θ_1 is the elastic angle of twist. The principle of virtual work for this beam can be written as

$$
\delta U = F_1\delta q_1(\ell) + M_1\delta\theta_1(\ell). \tag{4}
$$

The two governing equilibrium equations thus reduce to algebraic equations for the coupled extension-twist problem:

$$
\frac{\partial U_{1D}}{\partial \gamma_{11}} = F_1 \quad \frac{\partial U_{1D}}{\partial \kappa_1} = M_1 \tag{5}
$$

These equations are solved by using the first equation to eliminate γ_{11} in favor of F_1 and then using the second to express F_1 in terms of κ_1 and M_1, in order to enable comparison with theoretical results of Dancila et al. [14]. For constant k_1, the tip pretwist angle $\theta_0 = \ell k_1$, and κ_1 is also a constant so that the elastic tip twist angle $\theta = \ell\kappa_1$. The result is

$$
F_1 = \frac{-3A\ell M_1 + 12bN\theta(AD - B^2)}{[6B\ell - Ab^2(\theta + \theta_0)]} + \frac{2A^2b^5N\theta(\theta^2 + 3\theta_0\theta + 2\theta_0^2)}{15\ell^2[6B\ell - Ab^2(\theta + \theta_0)]} \tag{6}
$$

which reduces to the analytical result of Dancila et al. [14], for the special case of zero pretwist and antisymmetric layups, which has been validated with a geometrically nonlinear finite element analysis showing excellent correlation.

Non-zero pretwist and initial curvature as well as different layup configurations for the beam will continue to show negligible end effects, and the sixth row and column of the 1-D stiffness matrix continues to be zero. However, as also discussed by Yu et al. [63], this will lead to non-zero bending curvatures κ_2 and κ_3 since the bending will no longer be decoupled from extension and twist.

3.3. Applications to Z beams

The general results of the thin-walled open-section analysis are applied herein to beams with a "Z" cross section. Z sections present a very good case for extensive study of the trapeze effect because the bending in both directions is decoupled from the extension-twist problem, provided the flanges are identical. This is clearly observed when one browses through the expressions for those stiffness coefficients of general open sections, which contribute to this kind of a coupling. S_{13}, S_{14}, S_{23}, S_{24}, S_{35}, S_{45}, S_{36} and S_{46} are all odd functions of X_{n2} and X_{n3}. The anti-symmetric geometry of the Z section and identical flanges result in a cancellation of all coupling between bending and the other modes.

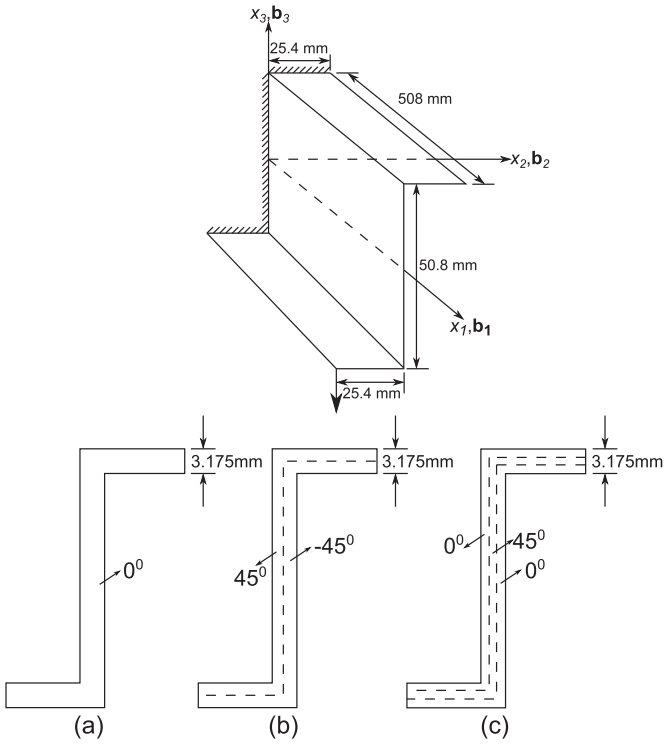

Fig. 7. Z-Section beam.

The layups considered by Gupta et al. [25] have the following material properties: $E_{11} = 206.8$ GPa, $E_{22} = 103.4$ GPa, $G_{12} = G_{13} = 51.7$ GPa and $\nu_{12} = 0.3$. Three cases as shown in Fig. 7 are considered:

- case (a): ply thickness =3.175 mm using the stacking sequence $[0°]_T$
- case (b): ply thickness =1.588 mm using the stacking sequence $[45°/-45°]_T$
- case (c): ply thickness =1.058 mm using the stacking sequence $[0°/45°/0°]_T$

For each case, a concentrated force of 4.45 N (hereafter referred to as the nominal load because 4.45 N = 1 lb) is applied at the tip of the lower flange as shown in the Fig. 7. OSBA is used to determine the numerical results for the deformation of the tip for the three cases.

The numerical results for the deflection and rotation of the tip, subjected to the nominal load, is presented in Tables 2 and 3, respectively. The results from the earlier works by Oden and Ripperger [41], Palani and Sundaramoorthy [43] and Gupta et al. [25] are also provided for comparison. Oden and Ripperger [41] derived analytical relations for warping, twist, and deflections of thin-walled, open-section beams assuming them to be purely isotropic. Palani and Sundaramoorthy [43] report finite element solutions again obtained from beam elements. Lateral displacements and twist are represented using first-order Hermite polynomials, while axial displacement is represented using a zeroth-order Hermite polynomial. Gupta et al. [25] report FE solutions obtained using 2-noded beam elements (with 8 degrees of freedom per node). First-order Hermite polynomials are used as interpolation functions for all degrees of freedom.

Table 2
Tip deflections of the Z-section beams at nominal load.

Tip deflections		Present work	Gupta et al. [25]	Palani et al. [43]	Oden [41]
u_1 (10^{-2} mm)	Case (a)	0	0	0	0
	Case (b)	0.00706	0.0162	0	0
	Case (c)	0	0	0	0
u_2 (10^{-2} mm)	Case (a)	1.549	1.44	1.469	1.44
	Case (b)	2.09	2.09	2.133	2.1
	Case (c)	1.7589	1.610	1.639	1.62
u_3 (10^{-2} mm)	Case (a)	−2.3233	−2.15	−2.19	−2.15
	Case (b)	−3.5579	−3.12	−3.187	−3.12
	Case (c)	−2.6384	−2.39	−2.449	−2.4

Table 3
Tip rotations of the Z-section beams at nominal load.

Tip rotations		Present work	Gupta et al. [25]	Palani et al. [43]	Oden [41]
θ_1 (10^{-5} rad)	Case (a)	57.02	56.6	53.2	56.7
	Case (b)	69.87	56.4	50.69	54.1
	Case (c)	61.78	58.4	52.3	58.5
q'_2(10^{-5} rad)	Case (a)	−6.86	−6.35	−6.48	−6.35
	Case (b)	−10.506	−9.21	−9.41	−9.23
	Case (c)	−7.7906	−7.07	−7.23	−7.09
q'^3 (10^{-5} rad)	Case (a)	4.57	4.26	4.34	4.27
	Case (b)	7.0028	6.19	6.298	6.2
	Case (c)	5.1937	4.75	4.84	4.77

Because of the assumed isotropy, the solutions from the relations in Oden and Ripperger [41] should only provide approximate solutions. The anisotropic / directional dependence is obviously not considered. However, the nonlinear and non-classical effects due to couplings are definitely absent. Both the works of Palani and Sundaramoorthy [43] and Gupta et al. [25] follow a similar approach of using Hermite interpolation polynomials to formulate a beam element for the finite element framework. This would mean that the displacement/rotations are being approximated by a polynomial of order n and thus the strains will be approximated by a polynomial of order $n-1$. Based on the earlier definition of asymptotic correctness, such an interpolation scheme might not capture all the terms of equal contribution. For example, in the work of Palani and Sundaramoorthy [43], the axial displacement is approximated by a zeroth-order Hermite polynomial (i.e., a linear polynomial), and thus the axial strain will be constant. However, other strains might not remain constant across the domain in all possible scenarios. Recovering the 2-D membrane strains and curvatures (See Eqs. (3) & (4) from Part-I) from the 1-D strains (and similarly the 3-D strains and stresses), the terms recovered will not be of correct order of magnitude. Even in the works of Gupta et al. [25], rotations are attributed as extra degrees of freedom leading to similar asymptotic incorrectness. As none of these three earlier works compared are asymptotically correct, even their linear solutions have some errors. In general, it could be said that these earlier works over-predict the stiffnesses, particularly the torsional stiffness. The over-prediction causes much larger errors for antisymmetric layups than for symmetric ones, as the stiffness reduction caused by cross-sectional in-plane warping in the former is larger. OSBA, which uses analytical solutions, provides reasonably accurate solutions at far less computational expense compared to standard finite elements formulations using beam elements.

With warping restrained at both fixed and free ends, the loads considered in the above cited works are very small for nonlinearities to make a significant difference. Hence, cases with one hundred times the nominal load were considered and compared with nonlinear FE results from Vo and Lee [57]. The resulting tip deflections and rotations are provided in Tables 4 and 5, respectively. The importance of nonlinear effects on the tip twist can be easily observed here. Vo and Lee [57] develop a general nonlinear beam element comprising all the axial-flexural-torsional couplings and implemented in a finite element framework. Thus, these results are much better equipped for comparison than the earlier three works. It is important to first note that the reference coordinate system used in Vo and Lee [57] is rotated in comparison to that defined in this work; see Figs. 2 & 3 from Part-I. In this work, the x_1-axis is defined along the length of beam while this is the x_3-axis in Vo and Lee [57]. Thus, changes have been made accordingly in order to properly interpret deflections and rotations (including signs) for comparison purposes. The main differences in the results can be seen in the axial and torsional modes. As can be seen in the theory of Vo and Lee [57], when warping is restrained, it restricted to zero; and when warping is free, the bi-moment is zero. However, in this work, restraining the warping at a free end restricts both the axial and warping displacements at the free end, hence resulting in $u_1 = 0$ for the cases of restrained warping, while no condition is imposed for the case of free warping (thus allowing all warping modes). The errors observed for θ_1 and U_1 are large, in comparison with the work of Vo and Lee [57]. However, as seen in Tables 2 and 3, the results match reasonably well. All the other quantities including the primary deformations (U_3, θ_2) and secondary deformation (U_2, θ_3) are within acceptable error limits. In addition, it is important to note that the same errors are also discussed by Vo and Lee [57]. Vo and Lee [57] propose and use a nonlinear beam model that can still contain errors.

As discussed in the earlier example on I-section with random layups, the results from this work match reasonably well with the shell-based FEM results. Yet, since VAM relies on asymptotic approximation of the overall energy, it is possible that additional orders of approximation (beyond second) are needed in certain cases. It is also possible that the beam models from Vo and Lee [57] do not consider all the necessary deformation modes. A through comparison with 3D Finite Element solutions will indeed serve to improve the trustworthiness of the

Table 4
Tip deflections of the Z-section beams at hundred times nominal load. All units are in mm.

		Free			Restrained		
		OSBA	Vo & Lee [57]	% Error	OSBA	Vo & Lee [57]	% Error
Case a	U_1	−0.028509	NA	NA	0	NA	NA
	U_2	−1.54896	NA	NA	−1.54896	NA	NA
	U_3	−2.32333	NA	NA	−2.32333	NA	NA
Case b	U_1	−0.0178374	−0.0069	158.5	0	−0.0127	NA
	U_2	−2.37161	−2.2718	4.393	−2.37161	−2.3392	1.386
	U_3	−3.5579	−3.1442	13.16	−3.5579	−3.3467	6.311
Case c	U_1	−0.053048	−0.0152	65	0	−0.0129	NA
	U_2	−1.75894	−1.8654	5.7	−1.75894	−1.8141	3.04
	U_3	−2.63841	−2.7162	1.91	−2.63841	−2.6690	0.55

Table 5
Tip rotations of the Z-section beams at hundred times nominal load. All units are in rad.

		Free			Restrained		
		OSBA	Vo & Lee [57]	% Error	OSBA	Vo & Lee [57]	% Error
Case a	θ_1	−0.2709	NA	NA	0.028509	NA	NA
	θ_2	−0.0068602	NA	NA	−0.0068602	NA	NA
	θ_3	−0.0045737	NA	NA	−0.0045737	NA	NA
Case b	θ_1	−0.486074	−0.0580	738	0.034932	0.0348	0.38
	θ_2	−0.0105057	−0.0089969	16.77	−0.0105057	−0.0097883	7.32
	θ_3	−0.00700277	−0.0068550	2.16	−0.00700277	−0.0069795	0.33
Case c	θ_1	−0.316613	−0.0631	400	0.0308899	0.0309	0.03
	θ_2	−0.0077906	−0.007803	1.32	−0.0077906	−0.007803	1.32
	θ_3	−0.0051937	−0.0056945	8.8	−0.0051937	−0.0054078	3.95

proposed solution. However, such a validation cannot be considered trivial and can be computationally expensive and thus beyond the scope of this present work.

New table for 100 times nominal load - Beam deflections. All units are in mm.

New table for 100 times nominal load - Beam rotations. All units are in rad.

The coordinate system used in Table 4 and 5 are as discussed in this work in Fig. 1.

4. Application to probabilistic analysis

Uncertainties in composite materials exist because of the material defects such as interlaminar voids, delamination, incorrect orientation, damaged fibers and variation in thickness. According to the nature and extent of uncertainty existing in the laminated composites, different approaches can be used. If the uncertainty is caused by the lack of precise information and/or statistical data that cannot be obtained, then the non-probabilistic approaches such as fuzzy sets can be used. On the other hand, if the uncertain parameters are treated as random variations with known probabilistic distributions, then the theory of probability or random process can be used. Probabilistic models can capture the influence of even unknown sources of uncertainty.

Several stochastic methods have been used to analyze an uncertain unsymmetrical laminated beam by integrating uncertain aspects into the finite element modeling. In the present work, we employ Monte Carlo methods to demonstrate the computational efficiency for simple stochastic analysis. The distributions employed for the material and geometric properties are given in Table 6.

In order to demonstrate the stochastic variance of the beam stiffness, tip deflections and rotations, we consider the I-section beam considered earlier. The geometric and material properties defined earlier can be considered as the mean values and the coefficient of variation is assumed to be 0.0574. A random number generation algorithm from MATLAB is utilized to generate datasets for material and geometric properties that corresponds to the distributions described in Table 6. The total size of the sample space for the results discussed below is 1,048,576.

Table 6
Properties and their probabilistic distributions.

Properties	Probabilistic distributions
Longitudinal modulus	Lognormal
Transverse modulus	Lognormal
Shear modulus	Lognormal
Poisson ratio	Truncated lognormal
Geometric properties	Gamma

The resulting distributions of plausible important stiffness measures (Extension, Twist, Bending, Extension-Twist coupling, Extension-Bending coupling, Twist-Bending coupling) are as given in Figs. 8 and 9.

Further on, using each of the resulting stiffness matrices, the 1-D nonlinear beam problem is solved for an applied load of 10 N at the tip of the bottom flange along the negative *y*-direction. The resulting distributions for plausible tip deflections and rotations are as shown in Fig. 10. The dispersion (or statistical dispersion) in the bending stiffness (S_{44}) is approximately about four times the minimum value of the bending stiffness and similar trend can be observed in the displacements and rotations. Thus, the resulting histograms seem reasonable.

Finally, the stochastic solutions are obtained for different sample space sizes and the resulting computational times are roughly calculated using the command *cputime* at the start and end of the simulation. Fig. 11 shows the variation of computational time with sample space size. Since each problem is independent of the other, the computational time varies almost linearly relative to the size of the sample space. It should be noted that each of the sample spaces chosen are independent of the other. Additionally, no adaptive scheme is used to find a suitable starting point for the iterations. Though in general the algorithm is expected to scale linearly, there could be potential instability points. However, when the number of points are increased, it is possible to encounter additional points where the algorithms could take longer to converge owing to the bad estimation of the starting point. The sudden jump in around 6×10^5 can be attributed to two aspects is likely to be attributed to this. In addition, OSBA is not an optimized code and written in a high-level language like MATLAB, as discussed below. This can cause changes in computational times of the order seen here. The goal of this section is to demonstrate the applicability of the method for large problems involving probabilistic scenarios. Further work on the scaling of the algorithm is definitely necessary and can be considered for future work.

It is important to understand that OSBA is built using a high-level language like MATLAB where programs would execute much slowly (compared to those written in compiled languages such as Fortran or C). Secondly, OSBA is not a completely optimized set of codes. There is scope for further optimization e.g., (a) to use the faster built-in MATLAB routines (as much as possible) or (b) pre-allocating all arrays prior to their utilization. In spite of the above drawbacks, it is important to note that sample space of more than one million could be computed in less than 4500 s.

5. Conclusions and future work

5.1. Conclusions

The theory presented in this work is part of an overall framework of tools under development for cross-sectional analysis of rotor blades and

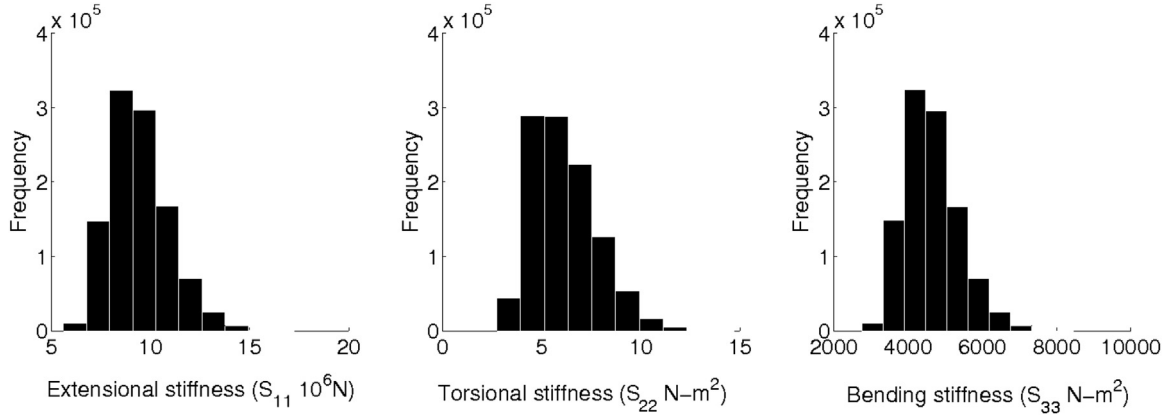

Fig. 8. Probabilistic distributions of stiffness matrix components: Extension (Left); Twisting (Middle); Bending κ_2 (Right).

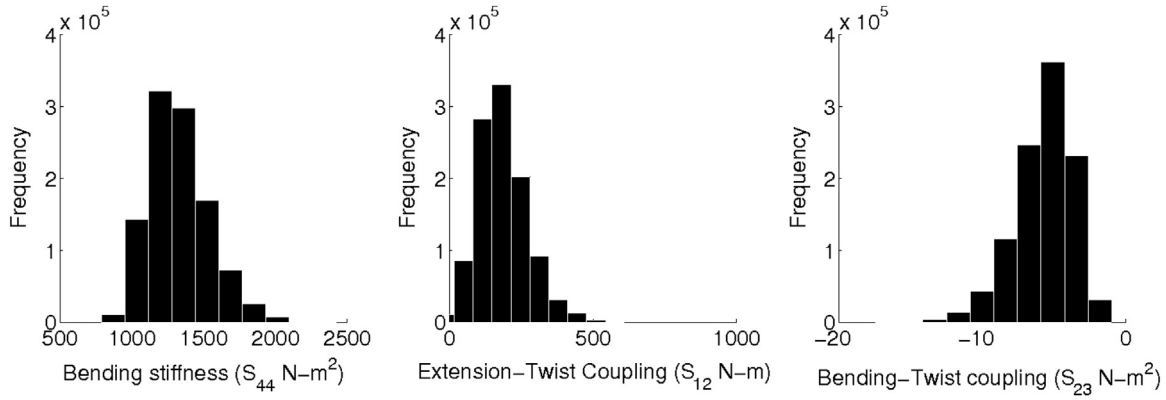

Fig. 9. Probabilistic distributions of stiffness matrix components: Bending κ_3 (Left); Extension-Twist (Middle); Bending-Twist (Right).

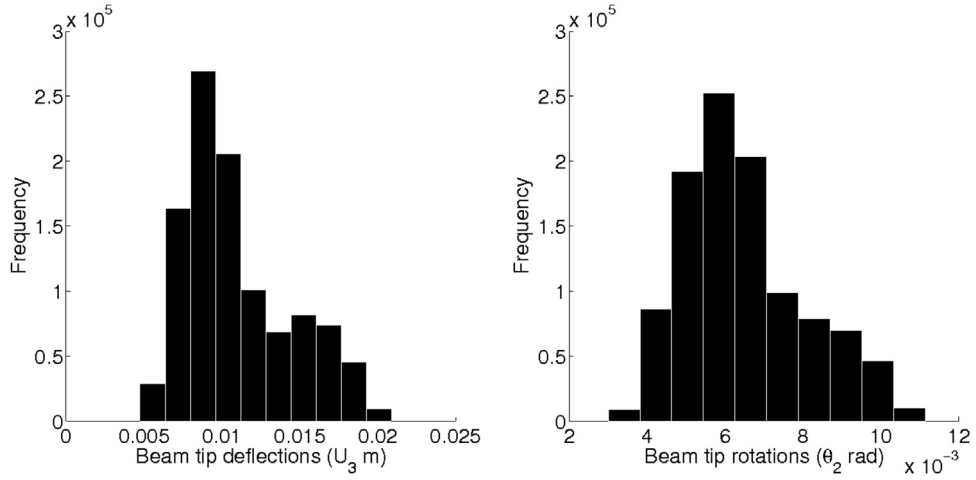

Fig. 10. Probabilistic distributions of possible beam tip deflections and rotations: deflection U_3 (Left) and rotation θ_2 (Right).

other slender, anisotropic structural members. The overall goals include development of finite element approaches for reduced arbitrary, built-up cross-sectional geometries and closed-form expressions for thin-walled cross sections with arbitrary geometry.

While targeting the nonlinear strain field phenomena in thin-walled composite beams, this work has resulted in the development of a unified theory in closed form, incorporating all the non-classical effects which contribute to the energy terms of the same order as the classical terms, due to the presence of small geometric parameters in the structures. Few approaches are available in the literature to analyze the nonlinear "trapeze effect" for anisotropic beams of arbitrary geometry. Since they are not based on asymptotic approaches, the asymptotical correctness of these analyses is difficult to assess.

The asymptotic analytical nonlinear, non-classical analysis of thin-walled open sections of reasonably arbitrary geometries, is accomplished by extending the theory developed for generally-anisotropic inclined strips pretwisted about an arbitrary reference line. The cross-sectional geometries analyzed are arbitrary assemblies of thin rectangles with rigid joints located anywhere along the two or more rectangles at each joint. The component strips could be of different widths, thicknesses, layups and materials. The assembly is then allowed a small pretwist about an arbitrary point in the cross section. All the non-classical nonlinear contributions that are of the same order as classical, linear contributions to the strain energy, including the trapeze

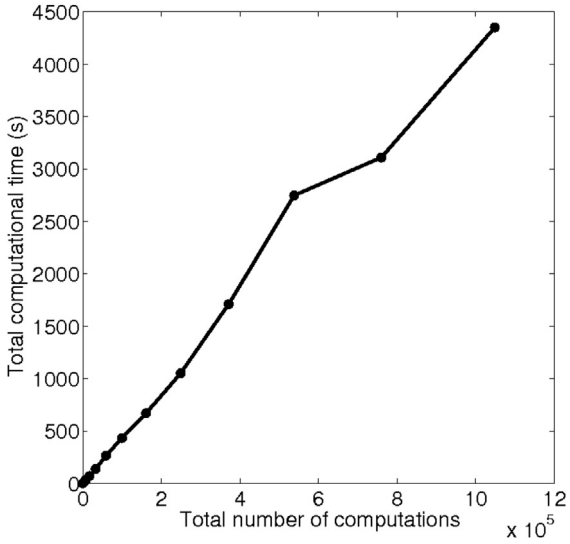

Fig. 11. Computational time as a function of sample space size.

and Vlasov effects, are captured asymptotically. Results are provided for the fully coupled non-classical beam stiffness, 3-D stresses and warping fields. Examples of beams with I-sections, star-sections, and Z-sections, made of laminated composites, are presented. Additionally results from simple Monte Carlo simulations are demonstrated to show the applicability of developed models for more extensive stochastic solutions. Comparisons are made with a few published linear and nonlinear results.

This work shows that the non-classical nonlinearities being brought into prominence in open-section beams are due to the thin walls which undergo large warping due to elastic twist. In general, this could be excited in any beam, because generally anisotropic materials are considered here. Thus, this work demonstrates a class transition from Class S to Class T beams by capturing the relevant non-classical nonlinearities analytically, and in an asymptotically-correct manner, for specific geometries.

5.2. Future work

The theoretical framework and the numerical tools developed for the open-section beams provides several facets for future exploration. Some notable improvements could include determination and study of the nonlinear, non-classical effects in single- and multi-cell beams with closed cross sections. During the manufacturing and curing process of composites, effects due to hygrothermal stresses would be of notable interest. The developed cross-sectional analysis holds true for dynamic analysis and could be used to develop closed-form solutions for simple cases like oscillating cantilever beams etc. Overall, the developed framework opens a plethora of opportunities to be explored.

References

[1] R.S. Barsoum, R.H. Gallagher, Finite element analysis of torsional and torsional-flexural stability problems, Int. J. Numer. Methods Eng. 2 (1970) 335–352.
[2] C. Basaglia, D. Camotim, N. Silvestre, Non-linear GBT formulation for open-section thin-walled members with arbitrary support conditions, Comput. Struct. 89 (2011) 1906–1919.
[3] N.R. Bauld, L.S. Tzeng, A vlasov theory for fiber-reinforced beams with thin-walled open cross-section, Int. J. Solids Struct. 20 (1984) 277–297.
[4] Z.P. Bazant, M.E. Nimeiri, Large deflection spatial buckling of thin-walled beam and frames, J. Eng. Mech. Div. 99 (1973) 1259–1281.
[5] J.P. Blasques, Optimal Design of Laminated Composite Beams (Ph.D. thesis), Technical University of Denmark, Kongens Lyngby, Denmark, 2011.
[6] J.P. Blasques, R.D. Bitsche, V. Fedorov, B.S. Lazarov, Accuracy of an efficient framework for structural analysis of wind turbine blades, Wind Energy 19 (2016) 1603–1621.
[7] J.P.A.A. Blasques, Multi-material topology optimization of laminated composite beams with eigenfrequency constraints, Compos. Struct. 111 (2014) 45–55.
[8] J.P.A.A. Blasques, R. Bitsche, An efficient and accurate method for computation of energy release rates in beam structures with longitudinal cracks, Eng. Fract. Mech. 133 (2015) 56–69.
[9] J.P.A.A. Blasques, M. Stolpe, Multi-material topology optimization of laminated composite beam cross-sections, Compos. Struct. 94 (2012) 3278–3289.
[10] L.F. Boswell, S.H. Zhang, The effect of distortion in thin-walled box-spine beams, Int. J. Solids Struct. 20 (1984) 845–862.
[11] J.B. Cardoso, A.J. Valido, Cross-section optimal design of composite laminated thin-walled beams, Comput. Struct. 89 (2011) 1069–1076.
[12] C.E.S. Cesnik, D.H. Hodges, VABS: A new concept for composite rotor blade cross-sectional modeling, J. Am. Helicopter Soc. 42 (1) (1997) 27–38.
[13] J.M.F. Cruz, A.V. Mendonca, Torsional analysis of thin-walled beams of open sections by the direct boundary element method, Comput. Struct. 136 (2014) 90–97.
[14] D. Dancila, K.I.B. Stefan, E.A. Armanios, Star-shape cross section extension-twist-coupled composite beams for rotorcraft applications, in: Proceedings of the 54th Annual National Forum of the AHS, Washington D. C., 1998, 1044–1048.
[15] J.F. Davalos, P.A. Qiao, Computational approach for analysis and optimal design of FRP beams, Comput. Struct. 70 (1999) 169–183.
[16] L. Feo, G. Mancusi, Modeling shear deformability of thin-walled composite beams with open cross-section, Mech. Res. Commun. 37 (2010) 320–325.
[17] G.J. Francois, Star beam, in: Proceedings of Shell and Spatial Structures Engineering, Proceedings of the International Symposium, Rio de Janerio, Brazil, 1984, 13–24.
[18] S. Gabriele, N. Rizzi, V. Varano, A 1d nonlinear twb model accounting for in plane cross-section deformation, Int. J. Solids Struct. 94–95 (2016) 170–178.
[19] G. Garceaa, R. Goncalvesb, A. Bilottaa, D. Manta, R. Bebianoc, L. Leonettia, D. Magisanoa, D. Camotimc, Deformation modes of thin-walled members: A comparison between the method of generalized eigenvectors and generalized beam theory, Thin Walled Struct. 100 (2016) 192–212.
[20] A. Genoese, A. Genoese, A. Bilotta, G. Garcea, Buckling analysis through a generalized beam model including section distortions, Thin Walled Struct. 85 (2014) 125–141.
[21] A. Genoese, A. Genoese, A. Bilotta, G. Garcea, A generalized model for heterogeneous and anisotropic beams including section distortions, Thin Walled Struct. 74 (2014) 85–103.
[22] V. Giavotto, M. Borri, G. Ghiringhelli, V. Carmaschi, G.C. Maffioli, F. Mussi, Anisotropic beam theory and applications, Comput. Struct. 16 (1989) 403–413.
[23] R. Goncalves, D. Camotim, On distortion of symmetric and periodic open-section thin-walled members, Thin-Walled Struct. 94 (2015) 314–324.
[24] R.K. Gupta, A. Venkatesh, K.P. Rao, Finite element analysis of laminated anisotropic thin-walled open-section beams, Compos. Struct. 3 (1985) 19–31.
[25] R.K. Gupta, A. Venkatesh, K.P. Rao, Finite element analysis of laminated anisotropic thin-walled open-section beams, Compos. Struct. 3 (1) (1985) 19–31.
[26] D.H. Hodges, Nonlinear Composite Beam Theory, American Institute of Aeronautics and Astronautics, 2006.
[27] D.H. Hodges, D. Harursampath, V.V. Volovoi, C.E.S. Cesnik, Non-classical effects in non-linear analysis of anisotropic strips, Int. J. Non-Linear Mech. 34 (2) (1999) 259–277.
[28] D.H. Hodges, R.A. Ormiston, D.A. Peters, On the Nonlinear Deformation Geometry of Euler-bernoulli Beams, NASA, 1980TP 1566.
[29] J. Høgsberg, S. Krenk, Analysis of moderately thin-walled beam cross-section by cubic isoparametric elements, Comput. Struct. 134 (2014) 88–101.
[30] M.Z. Kabir, A.N. Sherbourne, Optimal fiber orientation in lateral stability of laminated channel section beams, Composites B 29B (1998) 81–87.
[31] N. Kim, D.K. Shin, M.Y. Kim, Exact solutions for thin-walled open-section beams with arbitrary lamination subjected to torsional moment, Thin-Walled Struct. 44 (2006) 638–654.
[32] S.B. Kim, M.Y. Kim, Improved formulation for spatial stability and free vibration of thin-walled tapered beams and space frames, Eng. Struct. 22 (2000) 446–458.
[33] R.K. Kovvali, D.H. Hodges, Verification of the variational asymptotic beam section (VABS) analysis for initially curved and twisted beams, J. Aircr. 49 (3) (2012) 861–869.
[34] H.Y. Kwak, D.Y. Kim, H.W. Lee, Effect of warping in geometric nonlinear analysis of spatial beams, J. Constr. Steel Res. 57 (2001) 729–751.
[35] J. Lee, S.E. Kim, Flexural-torsional buckling of thin-walled i-section composites, Comput. Struct. 79 (2001) 987–995.
[36] J. Lee, S.H. Lee, Flexural-torsional behavior of thin-walled composite beams, Thin-Walled Struct. 42 (2004) 1293–1305.
[37] L. Li, Structural Design of Composite Rotor Blades With Consideration of Manufacturability, Durability and Manufacturing Uncertainties (Ph.D. thesis), Georgia Institute of Technology, Atlanta, Georgia, U.S.A., 2008.
[38] Z. Li, J.M. Ko, Y.Q. Ni, Torsional rigidity of reinforced concrete bars with arbitrary sectional shape, Finite Elem. Anal. Des. 35 (2000) 339–361.
[39] S. Murugan, R. Ganguli, D. Harursampath, Aeroelastic response of composite helicopter rotor with random material properties, J. Aircr. 45 (2008) 306–322.
[40] T.-T. Nguyen, P.T. Thang, J. Lee, Flexural-torsional stability of thin-walled functionally graded open-section beams, Thin Walled Struct. 110 (2017) 88–96.
[41] J.T., Oden, E.A. Ripperger, Mechanics of Elastic Structures, Hemisphere Pub. Corp., Washington and McGraw-Hill, New York, 1981.
[42] B. Omidvar, A. Ghorbanpoor, Nonlinear fe solution for thin-walled open-section composite beams, J. Struct. Eng. 122 (1996) 1369–1378.
[43] G.S. Palani, R. Sundaramoorthy, Finite element analysis of thin walled curved beams made of composites, J. Struct. Eng. 118 (8) (1992) 2039–2062.
[44] Y.L. Pi, M.A. Bradford, Effects of approximations in analyses of beams of open thin-

walled cross-section. Part II. 3d non-linear behavior, Int. J. Numer. Methods Eng. 51 (2001) 773–790.
[45] B. Popescu, D.H. Hodges, Asymptotic treatment of the trapeze effect in finite element cross-sectional analysis of composite beams, Int. J. Non-Linear Mech. 34 (1999) 709–721.
[46] R. Schrad, Verallgemeinerte Technische Biegetheorie, Springer Verlag, Berlin, Heidelberg, 1989.
[47] U. Schramm, V. Rubenchik, W.D. Pilkey, Beam stiffness matrix based on the elasticity equations, Int. J. Numer. Methods Eng. 40 (1997) 211–232.
[48] N. Silvestre, D. Camotim, Non-linear generalized beam theory for cold-formed steel members, Int. J. Struct. Stab. Dyn. 3 (2003) 461–490.
[49] N. Silvestre, D. Camotim, On the mechanics of distortion in thin-walled open sections, Thin-Walled Struct. 48 (2010) 469–481.
[50] K.S. Surana, Isoparametric elements for cross-sectional properties and stress analysis of beams, Int. J. Numer. Methods Eng. 14 (1979) 475–497.
[51] G. Turkalj, J. Brnic, J. Prpic-Orsic, Large rotation analysis of elastic thin-walled beam-type structures using ESA approach, Comput. Struct. 81 (2003) 1851–1864.
[52] A.J. Valifo, J.B. Cardoso, Geometrically nonlinear composite beam structures: design sensitivity analysis, Eng. Optim. 5 (2003) 531–551.
[53] A.J. Valifo, J.B. Cardoso, Geometrically nonlinear composite beam structures: Optimal design, Eng. Optim. 5 (2003) 553–561.
[54] V.Z. Vlasov, Thin Walled Elastic Beams, Moscow 1962.
[55] T.P. Vo, J. Lee, Flexural-torsional coupled vibration and buckling of thin-walled open-section composite beams using shear-deformable beam theory, Int. J. Mech. Sci. 51 (2009) 631–641.
[56] T.P. Vo, J. Lee, Geometrically nonlinear analysis of thin-walled open-section composite beams, Comput. Struct. 88 (2010) 347–356.
[57] T.P. Vo, J. Lee, Geometrically nonlinear analysis of thin-walled open-section composite beams, Comput. Struct. 88 (5–6) (2010) 347–356.
[58] X.X. Wu, C.T. Su, Simplified theory for composite thin-walled beams, AIAA J. 30 (1992) 2945–2951.
[59] Y.B. Yang, W. McGuire, Stiffness matrix for geometric nonlinear analysis, J. Struct. Eng. 112 (1986) 853–877.
[60] W. Yu, M. Blair, GEBT: A general purpose nonlinear analysis tool for composite beams, Compos. Struct. 94 (2012) 2677–2689.
[61] W. Yu, D.H. Hodges, J.C. Ho, Variational asymptotic beam sectional analysis - an updated version, Int. J. Eng. Sci. 59 (2012) 40–64.
[62] W. Yu, D.H. Hodges, V.V. Volovoi, C.E.S. Cesnik, On timoshenko-like modeling of initially curved and twisted composite beams, Int. J. Solids Struct. 39 (19) (2002) 5101–5121.
[63] W. Yu, V.V. Volovoi, D.H. Hodges, X. Hong, Validation of variational asymptotic beam sectional (VABS) analysis, AIAA J. 40 (10) (2002) 2105–2112.